January 1, 1984

Theory of plasma waves in the auroral E-region

Bela G. Fejer, *Utah State University*
J. Providakes
D. T. Farley

JOURNAL OF GEOPHYSICAL RESEARCH, VOL. 89, NO. A9, PAGES 7487–7494, SEPTEMBER 1, 1984

Theory of Plasma Waves in the Auroral *E* Region

BELA G. FEJER, JASON PROVIDAKES, AND DONALD T. FARLEY

School of Electrical Engineering, Cornell University, Ithaca, New York

We have extended the linear fluid theory of electrojet plasma waves to the region where ion magnetization effects are important. Our general dispersion relation includes the effect of cross-field and field-aligned drifts, ion inertia, electron density gradients, and recombination. In the absence of density gradients and recombinational damping, the oscillation frequency at marginal instability is changed by the ion magnetization effects from the ion acoustic frequency, $\omega = kC_s$, to the modified ion cyclotron frequency $\omega^2 = \Omega_i^2 + k^2C_s^2$. These upper *E* region waves can be driven by field-aligned and/or cross-field drifts and have the smallest threshold drift velocities at heights where electron-ion and/or anomalous electron collision frequencies are important. In the upper *E* region the most unstable wavelengths correspond to $k_\perp R_i \sim 1$, where R_i is the ion Larmor radius. Electron density gradients can increase or decrease considerably the threshold drift velocity for large-scale (a few tens of meters and larger) waves. Recombinational damping increases the threshold drift velocity for marginal instability of two-stream ion cyclotron waves and imposes a threshold drift velocity for the excitation of large-scale gradient drift waves propagating nearly perpendicular to the magnetic field. The effect of recombination is surprisingly important, even for wavelengths as short as 10–20 m, for altitudes at which $\nu_i \sim \Omega_i$. At these altitudes and above, the effect of even a very small $k_\parallel$ becomes increasingly important. The theory puts a number of earlier theoretical results together in one framework and provides new results and insights that may explain some puzzling observations such as those of Moorcroft (1979), who sometimes failed to see echoes with the 398-MHz Homer radar when the electric field measured with the Chatanika radar far exceeded the normal instability threshold.

INTRODUCTION

The theory of electrostatic plasma waves in the auroral electrojet has been described in a number of papers [e.g., *Ossakow et al.*, 1975; *Wang and Tsunoda*, 1975; *Fejer and Kelley*, 1980; *St.-Maurice and Schlegel*, 1983; *Keskinen and Ossakow*, 1983; *Hanuise*, 1983]. These instability theories are extensions of results derived initially for the equatorial electrojet, and they are valid only in the regime where the ions are unmagnetized ($\nu_i \gg \Omega_i$, where ν_i and Ω_i are the ion collision frequency and gyrofrequency). In the auroral electrojet, however, the ion gyrofrequency is about twice as large as at the equator, and the drift velocities also are frequently considerably larger. As a result the unstable layer in the auroral zone may extend above 120 km [e.g., *Pfaff et al.*, 1984] to altitudes at which ion magnetization effects are important. Furthermore, *D'Angelo* [1973] and *Chaturvedi* [1976] suggested that strong field-aligned drifts should be able to excite collisional ion cyclotron waves in the upper (above about 120 km) auroral *E* region. Their theories, however, did not show how the transition between the electrojet and ion cyclotron waves takes place.

The main purpose of this paper is to develop a general theory which encompasses both electrojet waves (two stream and gradient drift) and waves observed at higher altitudes (ion cyclotron and current convective waves). To do this, we extend the electrojet instability theories to include the effect of the magnetic field on the ions and also the effect of field-aligned currents. The well-known electrojet waves and the results presented at *D'Angelo* [1973] and *Chaturvedi* [1976] are recovered as limiting cases. In this framework, ion cyclotron waves are generated by the two-stream instability at heights and wavelengths for which ion magnetization effects are dominant. Depending upon the wavelength being considered, the threshold drift velocity (field aligned and/or perpendicular to **B**) at which instability occurs can be affected substantially by electron density gradients, recombination, and electron-ion collisions.

Paper number 4A0706.
0148-0227/84/004A-0706$05.00

GENERAL DISPERSION RELATION

To derive the fluid dispersion relation for electrostatic plasma waves in the electrojet region, including ion magnetization, electron density gradient, and recombination effects, we start with the ion and electron continuity equations,

$$(\partial N/\partial t) + \nabla \cdot (N\mathbf{V}) = Q - \alpha N^2 \tag{1}$$

the two equations of motion,

$$m\frac{D\mathbf{V}}{Dt} = q(-\nabla\phi + \mathbf{V} \times \mathbf{B}) - \frac{\nabla P}{N} - m\nu\mathbf{V} \tag{2}$$

and Poisson's equation

$$\nabla^2\phi = e(N_e - N_i)/\varepsilon_0 \tag{3}$$

where Q and α are the production and recombination rates, D/Dt is the convective derivative, and the other symbols have their usual meaning. We assume the electron and ion collision frequencies with neutrals to be dominant (the effect of electron-ion collisions will be discussed later) and neglect electron inertia, neutral winds, and electric field shear effects. The equilibrium configuration with the ambient electric and magnetic fields and electron density gradient is shown in Figure 1. Following, for example, the procedure given in the work by *Sudan et al.* [1973] or *Fejer et al.* [1975], we next linearize these equations, assume quasi-neutrality (we are interested in waves with scale sizes much larger than the Debye length), and assume that the perturbations are proportional to $\exp[i(\mathbf{k} \cdot \mathbf{r} - \omega t)]$ in the reference frame of the ions. The details of the derivation are given in the appendix.

One version of the resulting dispersion relation for nearly field-aligned ($k_\perp \gg k_\parallel$) electrojet irregularities can be written as

$$[\nu_i - i(\omega - \Omega_i/kL_N)](\bar{\omega} - \mathbf{k} \cdot V_d) + \{\bar{\omega}[\Omega_i^2 + (\nu_i - i\omega)^2] + ik^2C_s^2[\nu_i - i(\omega - \Omega_i/kL_N)]\}\left(\frac{\psi}{\nu_i} - \frac{i}{kL_N\Omega_i}\right) = 0 \tag{4}$$

where $\mathbf{V}_d = \mathbf{V}_e - \mathbf{V}_i$ is the total (cross-field and field-aligned)

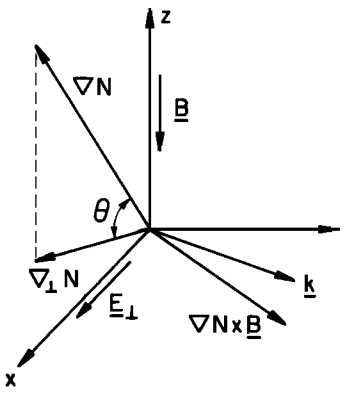

Fig. 1. Coordinate system used for the ambient electric and magnetic fields and electron density gradient. Here $\nabla_\perp N$ is the density gradient component perpendicular to the magnetic field. For a horizontally stratified ionosphere the angle θ between the ambient electron density gradient and the plane perpendicular to **B** is the magnetic dip angle.

drift velocity given in (A6), $\bar{\omega} = \omega + i2\alpha N_0$,

$$\psi = (\nu_e\nu_i/\Omega_e\Omega_i)(1 + \Omega_e{}^2k_\parallel{}^2/\nu_e{}^2k^2)$$

C_s is the ion acoustic speed, $L_N = N \sec\theta(\partial N/\partial h)^{-1}$ is the characteristic length of the electron density gradient in the direction perpendicular to **B**, and we have set **k** parallel to $\nabla N \times \mathbf{B}$ for simplicity. For a more general **k**, L_N must be replaced by $L_{\text{eff}} = k_\perp BN/[\mathbf{k}\cdot(\nabla N \times \mathbf{B})]$, as shown in the appendix (A5). This fluid theory is valid for wavelengths much larger than the ion mean free path or the ion Larmor radius R_i, whichever is smaller. Here we assume an isothermal plasma with identical electron and ion temperatures so that $R_i = C_s/\Omega_i$. For $k_\parallel \neq 0$ we also must have $\nu_e > k_\parallel(KT_e/m_i)^{1/2}$ (collisional electron case); i.e., the parallel component of the wavelength must be much larger than the electron mean free path.

In the following section we discuss initially the solutions of the dispersion relation at electrojet altitudes (between about 95 and 115 km), where ion cyclotron effects are negligible. We recover well-known results but emphasize more than usual the importance of recombination. Then we consider the more general solution which includes the effect of ion magnetization and is valid in the upper E region (above about 120 km). All numerical calculations shown in the figures to be presented were done using (4), without the approximations we shall make in the sections to follow.

Waves at Electrojet Altitudes

In this region the ions are unmagnetized and the relative drift velocity $\mathbf{V}_d$ is $\mathbf{E} \times \mathbf{B}/B^2$, approximately, since $\nu_i \gg \Omega_i$ and $\Omega_e \gg \nu_e$; i.e., to zero order the ions are at rest, and the electrons are collisionless. In this case the dispersion relation (4) reduces to

$$\bar{\omega} - \mathbf{k}\cdot\mathbf{V}_d + [\bar{\omega}(\nu_i - i\omega) + ik^2C_s{}^2]\left(\frac{\psi}{\nu_i} - \frac{i}{kL_N\Omega_i}\right) = 0 \qquad (5)$$

This is the well-known fluid dispersion relation for electrojet instabilities [e.g., *Sudan et al.*, 1973] except for the inclusion of recombinational damping in the $\bar{\omega}$ term. (The Ω_i in (5) appears even when magnetic effects are neglected in the ion momentum equation.) For unmagnetized ions the fluid theory is valid for $\nu_i{}^2 > \omega_r{}^2$, in other words, for wavelengths much larger than the ion mean free path (i.e., a few meters). For shorter wavelengths and/or drift velocities much larger than C_s, kinetic theory is required [e.g., *Farley*, 1963; *Ossakow et al.*, 1975; *Moorcroft*, 1979; *Schlegel*, 1983; *St.-Maurice and Schlegel*, 1983].

Assuming $\omega = \omega_r + i\Gamma$ with $\Gamma \ll \omega_r$, and $kL_N \gg \nu_i/[\Omega_i(1 + \psi)]$, the oscillation frequency and growth rate obtained from (5) are given by

$$\omega_r = \mathbf{k}\cdot\mathbf{V}_d/(1 + \psi) \qquad (6)$$

$$\Gamma = \frac{1}{1+\psi}\left[\frac{\psi}{\nu_i}(\omega_r{}^2 - k^2C_s{}^2) + \frac{\omega_r\nu_i}{kL_N\Omega_i}\right] - 2\alpha N_0 \qquad (7)$$

a result given in the work by *Fejer et al.* [1975] for plasma irregularities in the equatorial electrojet. In the rest frame the oscillation frequency is given by $\omega_r{}^* = (\mathbf{k}\cdot\mathbf{V}_e + \psi\mathbf{k}\cdot\mathbf{V}_i)/(1 + \psi)$. In the opposite limit of $kL_N < \nu_i/[\Omega_i(1 + \psi)]$ and $\Gamma \sim \omega_r$, the dispersion relation (5) gives the oscillation frequency and growth rate of the large-scale (λ of the order of a few kilometers) waves discussed by *Kudeki et al.* [1982] but not here. Near the center of the electrojet scattering region (about 100–115 km), $\mathbf{V}_d = \mathbf{E} \times \mathbf{B}/B^2$, and the electron density gradient is destabilizing (stabilizing) when $\mathbf{E}\cdot\nabla N$ is positive (negative). In the more general case, the electron density gradient is destabilizing (stabilizing) when $\mathbf{k}\cdot\mathbf{V}_d$ and $\mathbf{k}\cdot(\nabla N \times \mathbf{B})$ have the same (opposite) sign. Note that our local theory neglects velocity shear effects [e.g., *Huba et al.*, 1983]. For simplicity, we will consider in detail only waves propagating parallel to $\nabla N \times \mathbf{B}$.

The threshold drift velocity for instability (i.e., for which $\Gamma = 0$) implied by (7) is

$$\mathbf{k}\cdot\mathbf{V}_d = kC_s(1 + \psi)\left\{\left[F^2 + 1 + \frac{2\alpha N_0\nu_i(1+\psi)}{k^2C_s{}^2\psi}\right]^{1/2} - F\right\} \qquad (8)$$

where

$$F = \nu_i{}^2/2\Omega_ik^2C_sL_N\psi$$

This result, which was given in the work by *Farley and Fejer* [1975] except for the recombination term, shows explicitly how the gradient term can stabilitize or destabilize the plasma depending on the sign of L_N.

Figure 2 shows the variation with wavelength and electron density scale length of the normalized drift velocity ($\mathbf{k}\cdot\mathbf{V}_d/kC_s$) for marginal instability at 105 km obtained from the full dispersion relation (4) for $k_\parallel = 0$, assuming $\nu_e = 4 \times 10^4$ s^{-1}, $\nu_i = 2.5 \times 10^3$ s^{-1}, $\Omega_e = 10^7$ s^{-1}, $\Omega_i = 180$ s^{-1}, $C_s = 360$ m s^{-1}, and $2\alpha N_0 = 0.06$ s^{-1}, based on $\alpha = 3 \times 10^{-7}$ cm^{-3} s^{-1} [*Watt et al.*, 1974] and an electron density of 10^5 cm^{-3}. For these parameters we could equally well have used (5). Figure 2 also shows how recombinational damping increases the threshold velocity for the pure two-stream instability ($L_N = \infty$) at long wavelengths, as indicated by (8). These results indicate that large-scale (several tens of meters and larger) waves with **k** perpendicular to the magnetic field can be generated only in the presence of destabilizing electron density gradients if the electron density is large. For such waves, with $F \gg 1$, (8) reduces to $V_d = 2\alpha N_0L_N(\Omega_i/\nu_i)(1 + \psi)^2$. As was mentioned previously, *Kudeki et al.* [1982] have shown that for wavelengths of a few kilometers, the oscillation frequency and growth rate given in (6) and (7) are not valid and more general formulas, derived from (5), must be used.

The effects of the electron density gradient and recombination on the threshold drift velocity decrease rapidly as the aspect angle (angle between the wave vector and the magnetic field) decreases from 90° because of the rapid increase of ψ with $k_\parallel$. Figure 3 illustrates this variation for two given wavelengths for the parameters given above. For waves with $k_\parallel/k \gg \nu_e/\Omega_e \simeq 4 \times 10^{-3}$ at 105 km, diffusion along the field lines is the main damping mechanism. Note that for a stabilizing density gradient (dashed curves), the threshold velocity for instability is actually smaller when $k_\parallel \neq 0$, particularly for wavelengths larger than a few tens of meters. This is because the increase in ψ reduces the stabilizing effect of a negative F in (8) or, in physical terms, the increased parallel diffusion partially destroys the gradient drift effect. In addition, it can be shown from (6) and (7) that when the electron drift velocity is somewhat larger than the ion acoustic speed, the growth rate for wavelengths smaller than a few tens of meters maximizes for $k_\parallel \neq 0$ because of the ψ in the numerator of (7). The reason for this is that with $k_\parallel$ not exactly equal to zero, charge neutrality can be maintained by electron motion along the field lines. This variation of the growth rate with aspect angle has been studied by a number of authors using kinetic equations [e.g., *Wang and Tsunoda*, 1975; *Ossakow et al.*, 1975; *Schlegel and St.-Maurice*, 1982] but neglecting gradients and recombination.

WAVES ABOVE THE ELECTROJET

Let us now consider solutions of the more general dispersion relation (4) which we must use at altitudes where ion magnetization effects are important ($\Omega_i \gtrsim \nu_i$). Using $\Gamma \ll \omega_r, \nu_i$, the real part of the dispersion relation, obtained from (4), is given by

$$\omega_r - \mathbf{k}\cdot\mathbf{V}_d + \frac{\psi\omega_r}{\nu_i^2}(\Omega_i^2 + k^2C_s^2 + \nu_i^2 - \omega_r^2) + \frac{1}{kL_N\Omega_i}\cdot\left[-2\omega_r^2 + k^2C_s^2\left(-\frac{\psi\Omega_i^2}{\nu_i^2}\right)\right] + (\Gamma + 2\alpha N_0)(1 + 2\psi)\frac{\omega_r}{\nu_i} \simeq 0 \qquad (9)$$

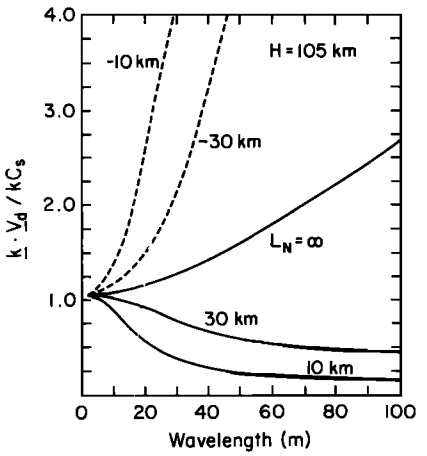

Fig. 2. Variation of the normalized threshold ($\Gamma \to 0$) drift velocity, with wavelength and electron density scale length for waves propagating perpendicular to the background magnetic field at 105 km with a recombination rate $2\alpha N_0 = 0.06\ s^{-1}$. The solid (dashed) curves correspond to the cases for which the electric field is parallel (antiparallel) to the electron density gradient.

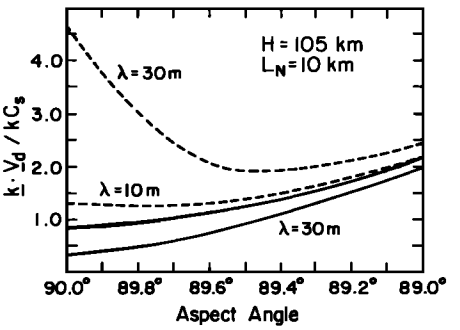

Fig. 3. Variation of the threshold drift velocity with aspect angle at 105 km with a recombination rate of 0.06 s^{-1}. The solid and dashed curves correspond to destabilizing and stabilizing electron density gradients, respectively.

and the imaginary part is

$$(\omega_r - \mathbf{k}\cdot\mathbf{V}_d)\left(\omega_r - \frac{\Omega_i}{kL_N}\right) + 2\omega_r^2\psi - k^2C_s^2\psi + \frac{1}{kL_N}\left[\frac{\omega_r}{\Omega_i}(\Omega_i^2 + \nu_i^2 - \omega_r^2) + k^2C_s^2\left(\frac{\omega_r}{\Omega_i} - \frac{1}{kL_N}\right)\right] - \nu_i(\Gamma + 2\alpha N_0)\left[1 + \frac{\psi}{\nu_i^2}(\Omega_i^2 + k^2C_s^2 + \nu_i^2 - \omega_r^2)\right] \simeq 0 \qquad (10)$$

assuming that $\nu_i \gg 2\alpha N_0$. These two equations determine ω_r and Γ. Above the electrojet region the fluid theory is valid only for $kR_i < 1$, i.e., $\lambda \gtrsim 15$–20 m, since the ion Larmor radius $R_i \sim 3$ m.

For $k_\parallel/k < \nu_e/\Omega_e$, $\psi \ll 1$ at these altitudes, and so $\omega_r \cong \mathbf{k}\cdot\mathbf{V}_d$, since all the other terms in (9) are negligible. In the rest frame we then have $\omega_r^* = \omega_r + \mathbf{k}\cdot\mathbf{V}_i \cong \mathbf{k}\cdot\mathbf{V}_e$. In other words, above the electrojet region the plasma waves which propagate perpendicular to the magnetic field are directly coupled to the **E** × **B** drift of the electrons even though they are driven by the ion Pedersen drift. For the opposite limit of $k_\parallel/k \gg \nu_e/\Omega_e$, the oscillation frequency will change considerably with altitude, as we shall see.

It is now convenient to substitute the value of $\omega_r - \mathbf{k}\cdot\mathbf{V}_d$ from (9) into (10) to obtain an expression for the growth rate as a function of the oscillation frequency. Retaining only the dominant terms, this result is

$$\Gamma \cong -2\alpha N_0 + \left\{\frac{\psi}{\nu_i^2}[\omega_r^4 - \omega_r^2(\Omega_i^2 + k^2C_s^2 - \nu_i^2) - \nu_i^2k^2C_s^2] + \frac{\omega_r}{kL_N\Omega_i}(\Omega_i^2 + \nu_i^2)\left[1 + \psi\frac{\Omega_i^2}{\nu_i^2}\right]\right\} \cdot \left\{\nu_i\left[1 + \frac{\omega_r^2}{\nu_i^2} + \frac{\psi}{\nu_i^2}(\Omega_i^2 + k^2C_s^2 + \nu_i^2 + \omega_r^2)\right]\right\}^{-1} \qquad (11)$$

In order to understand better the physics of the instability, we need simpler versions of these general results, and hence we now make further approximations.

Waves in the Absence of Gradients

If, for the moment, we neglect electron density gradients ($L_N \to \infty$) and recombinational damping ($\alpha \to 0$), we find from (11) that at marginal instability ($\Gamma \to 0$),

$$\omega_r^2[\omega_r^2 - (\Omega_i^2 + k^2C_s^2)] + \nu_i^2(\omega_r^2 - k^2C_s^2) = 0 \qquad (12)$$

in the reference frame of the ions. This result for ω_r is valid for

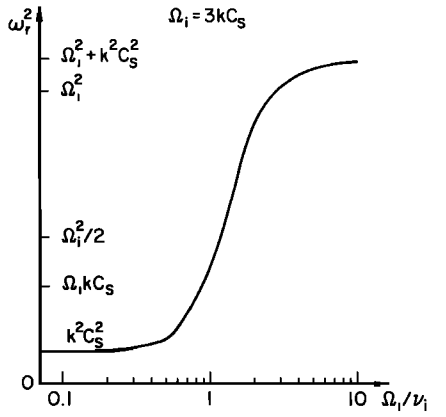

Fig. 4. Plot of the variation of the oscillation frequency of the two-stream ion cyclotron waves at marginal instability as a function of Ω_i/ν_i.

waves driven by either cross-field or field-aligned drifts. As a check, we can see that in the center of the electrojet region, where $\nu_i \gg \Omega_i$, kC_s, ω_r, (12) reduces to the well-known two-stream phase velocity $\omega_r = kC_s$, which also, of course, follows from (7). In the opposite limit at altitudes where $\Omega_i^2 \gg \nu_i^2$, we recover the oscillation frequency given by *D'Angelo* [1973] and *Chaturvedi* [1976] for collisional ion cyclotron waves, i.e., $\omega_r^2 = \Omega_i^2 + k^2C_s^2$. The transition from the unmagnetized to the magnetized limit is illustrated in Figure 4 for the case $\Omega_i = 3kC_s$.

The threshold drift velocity for marginal instability can be obtained from (10) with $\Gamma = \alpha = 0$, $L_N = \infty$; i.e.,

$$\mathbf{k} \cdot \mathbf{V}_d = \omega_r[1 + \psi(2 - k^2C_s^2/\omega_r^2)] \tag{13}$$

with ω_r given by (12). Since $\omega_r^2 > k^2C_s^2$, this result reduces to $\mathbf{k} \cdot \mathbf{V}_d \sim \omega_r$ for the most easily excited waves ($k_\parallel = 0$), for which $\psi \ll 1$ at these altitudes. In the limit $\omega_r = kC_s$, this threshold is independent of wavelength, but at higher altitudes where $\omega_r^2 = \Omega_i^2 + k^2C_s^2$, the threshold velocity will increase with increasing wavelength in the regime $\Omega_i^2 > k^2C_s^2$ (i.e., $kR_i < 1$). For wavelengths smaller than R_i, kinetic theory shows that the threshold will also increase. Hence we anticipate that above about 120 km where $\Omega_i > \nu_i$, the minimum threshold will occur for $kR_i \sim 1$ ($\lambda \sim$ 10–20 m), a result confirmed by kinetic theory calculations (J. Providakes, unpublished result, 1983). In other words, long-wavelength irregularities will not be excited in the absence of sharp electron density gradients.

Recombination, which we have neglected until now at these altitudes, in fact is often not negligible and increases the threshold velocity just as at lower altitudes. Figure 5 illustrates the increase for $\mathbf{k} \perp \mathbf{B}$ at about 122 km where $\Omega_i/\nu_i = 1$, $\Omega_e = 10^7$ s^{-1}, $\nu_e = 3.9 \times 10^3$ s^{-1}, $C_s = 430$ m s^{-1}, and $2\alpha N_0 = 0.04$ s^{-1}. For the recombination time we have used the coefficient α given by *Watt et al.* [1974] and an electron density of 10^5 cm^{-3}. When $\mathbf{k}$ is not perpendicular to $\mathbf{B}$ (i.e., $k_\parallel/k > \nu_e/\Omega_e$), however, ψ can be large, and parallel diffusion dominates recombination except for very long wavelengths.

The E region waves discussed here can be driven by cross-field or field-aligned drifts, as pointed out by *Chaturvedi* [1976], since the driving terms vary with powers of $\mathbf{k} \cdot \mathbf{V}_d = \mathbf{k} \cdot \mathbf{V}_\perp + k_\parallel V_\parallel$. However, the cross-field drift of the electrons relative to the ions decreases with the increase of ion magnetization, and it also rotates closer to the direction of the ion Pedersen drift (i.e., $\mathbf{V}_d \cong -(\nu_i/\Omega_i)\mathbf{E}/B_0$ for $\Omega_i/\nu_i \gg 1$); i.e., the current is primarily an ion Pedersen current. Therefore very large perpendicular electric fields are needed for the excitation of two-stream ion cyclotron waves well above the height where $\nu_i/\Omega_i = 1$ in the absence of field-aligned drifts. As a result, in the absence of sharp electron density gradients, field-aligned drifts are probably the prime source of free energy for the excitation of auroral waves above about 130 km.

In view of this, let us now consider the case $V_\perp = 0$ and $\Omega_i \gg \nu_i$. The threshold field-aligned drift velocity for instability obtained from (13) is then given by

$$V_\parallel \cong \frac{(\Omega_i^2 + k^2C_s^2)^{1/2}}{k_\parallel}\left[1 + \psi\left(\frac{2 + k^2R_i^2}{1 + k^2R_i^2}\right)\right] \tag{14}$$

Since $\nu_e\nu_i/\Omega_e\Omega_i \ll 1$, we have $1 + \psi \simeq 1 + \Omega_e\nu_i k_\parallel^2/\nu_e\Omega_i k^2$, and the minimum threshold velocity is given by

$$V_\parallel \cong \frac{2\Omega_i}{k}[(2 + k^2R_i^2)(\Omega_e\nu_i/\Omega_i\nu_e)]^{1/2} \tag{15}$$

for

$$\frac{k_\parallel}{k} = \left[\frac{\nu_e\Omega_i}{\Omega_e\nu_i}\frac{1 + k^2R_i^2}{2 + k^2R_i^2}\right]^{1/2}$$

Most of the preceding upper electrojet results were obtained for $kR_i \ll 1$. Assuming that the fluid theory is still reasonably valid for $kR_i = 1$ (i.e., $k = \Omega_i/C_s$), the minimum threshold drift velocity becomes

$$V_\parallel = 2\sqrt{3}\, C_s(\Omega_e\nu_i/\Omega_i\nu_e)^{1/2} \tag{16}$$

In this case, the minimum threshold drift velocity and the corresponding aspect angle $k_\parallel/k$ are proportional to $m_i^{-1/4}$, whereas the corresponding wavelength is proportional to $m_i^{1/2}$. Thus in a plasma with multiple ion species the ion cyclotron waves of the lightest ion species will have their minimum threshold at the shortest wavelength and largest aspect angle. Calculations of the threshold drift velocity using kinetic theory (J. Providakes, unpublished result, 1983) indicate a good agreement with (15) for $kR_i < 1$.

The minimum threshold velocities in (15) and (16) are proportional to $(\nu_i/\nu_e)^{1/2}$. Below about 130 km, in the absence of anomalous electron collisions ("collisions" with waves, i.e., nonlinear effects), $\nu_e = \nu_{en}$, and ν_e/ν_i is about 20 and does not change much with altitude. The minimum threshold field-aligned drift, for a height of about 130 km and $C_s = 500$ m s^{-1}, is $V_\parallel \simeq 90$ km s^{-1} for $kR_i = 1$ ($\lambda \simeq 17$ m). This drift velocity is comparable to the electron thermal speed. At altitudes where ν_{ei} becomes important we must replace ν_e and ψ

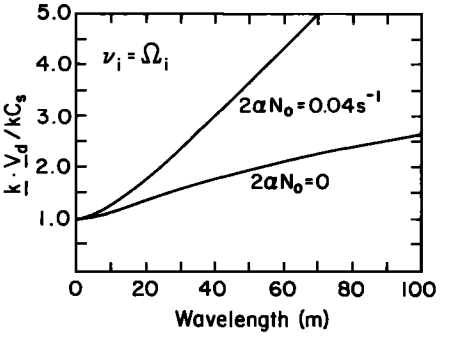

Fig. 5. Plot of the threshold drift velocity for waves propagating perpendicular to the magnetic field in a plasma with no electron density gradient at 122 km, where $\Omega_i = \nu_i$. These results are not accurate for wavelengths smaller than about 20 m.

by slightly more complicated functions. The effect of electron-ion collisions is to decrease the relative importance of parallel diffusion and to increase ν_e/ν_i. We will not deal with this topic in detail here, but in the simplest limit one simply replaces ν_e by $\nu_e = \nu_{en} + \nu_{ei}$. The effective electron collision frequency would be further increased in the presence of anomalous wave-particle collisions [e.g., *Sudan*, 1983].

In the fully ionized case, there are additional destabilizing effects due to electron thermal conductivity and viscosity [*Chaturvedi and Kaw*, 1975]. These effects should be important above about 150 km, where electron-ion collisions are dominant. Let us assume that these effects can be taken into account using an enhanced electron collision frequency. For example, for a height of about 150 km, using $\nu_i = 10\ s^{-1}$, $\nu_e = 4000\ s^{-1}$, and $C_s = 550\ m\ s^{-1}$, we get a minimum field-aligned drift $V_{\parallel} \simeq 19\ km\ s^{-1}$ with $kR_i = 1$ ($\lambda \simeq 19$ m) for NO^+ or O_2^+ ion cyclotron waves. For O^+ waves the wavelength for $kR_i = 1$ is about 14 m. The ratio of the ion to the electron collision frequency will continue to decrease with altitude, which implies a decreasing threshold drift velocity and an increasing $k_{\parallel}$. However, the modified collisional ion cyclotron theory discussed here is valid only for $\nu_e > k_{\parallel} V_{Te}$, i.e., when the parallel component of the wavelength is larger than the electron mean free path.

So far we have discussed only marginal instability conditions. We can determine the oscillation frequency for velocities larger than the threshold drift by examining (9) and (11). Again, we first neglect recombinations and gradient effects, in which case (11) becomes

$$\omega_r^2 \cong \Omega_i^2 + k^2C_s^2 - \nu_i^2(1 - k^2C_s^2/\omega_r^2) + \Gamma\nu_i\left[\frac{1}{\psi}(1 + \nu_i^2/\omega_r^2) + (\Omega_i^2 + k^2C_s^2 + \nu_i^2 + \omega_r^2)/\omega_r^2\right] \tag{17}$$

For altitudes where Ω_i, $\omega_r \gg \nu_i$, the smallest field-aligned threshold drift velocity occurs for $\psi \sim 1$, and a large increase in Γ corresponds to only a small change in ω_r. Therefore the oscillation frequency will remain equal to the marginal instability value ($\omega_r^2 \simeq \Omega_i^2 + k^2C_s^2$). In this case, for $L_N = \infty$, it can be shown from (9) that the growth rate is proportional to $\mathbf{k} \cdot \mathbf{V}_d$. On the other hand, for $k_{\parallel}/k < \nu_e/\Omega_e$, $\psi \ll 1$, and the oscillation frequency is proportional to the drift velocity even at higher altitudes, as has been discussed previously. We can see from (17) that for $\Omega_i \gg \nu_i$, the transition between the two regimes occurs for $\psi \sim \nu_i^2/\Omega_i^2$, i.e., for $k_{\parallel}/k \simeq (\nu_e\nu_i/\Omega_e\Omega_i)^{1/2}$.

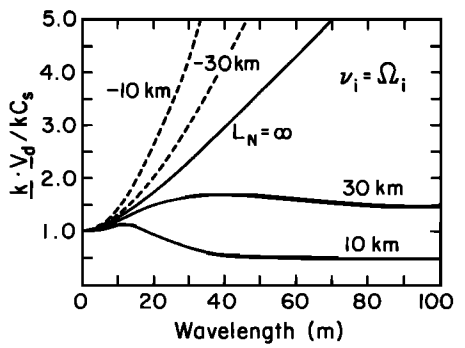

Fig. 6. Normalized threshold drift velocity for waves with **k** perpendicular to the magnetic field at 122 km. The recombination rate $2\alpha N_0$ was assumed to be $0.04\ s^{-1}$. These results are not accurate for wavelengths smaller than about 20 m.

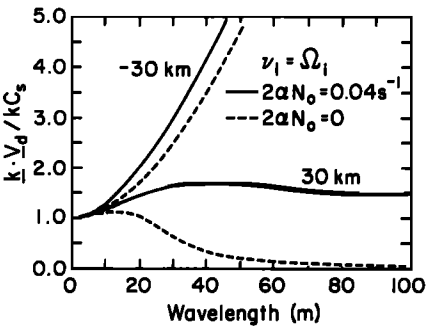

Fig. 7. Example of the effect of recombinational damping on the threshold drift velocity for waves perpendicular to the magnetic field. The upper (lower) curves correspond to a stabilizing (destabilizing) electron density gradient.

These last results indicate that E region ion cyclotron waves are most likely to be generated by field-aligned currents where $\Omega_i \gg \nu_i$ and where the effective electron collision frequency is much higher than the electron-neutral collision frequency. The auroral electric fields perpendicular to **B** are never strong enough to excite these two-stream ion cyclotron waves where $\Omega_i \gg \nu_i$. At lower altitudes the field-aligned threshold drift velocity is considerably larger, and the oscillation frequency is proportional to the drift velocity for waves driven by both cross-field and field-aligned drifts. That is, at lower altitudes the cyclotron resonance is destroyed by ion-neutral collisions.

Electron Density Gradient Effects

The threshold drift velocity of long-wavelength waves is affected considerably by electron density gradient effects, as at lower altitudes where we neglected ion magnetization effects. The importance of the gradient can be easily estimated from (11) by comparing the ion inertial terms (the first two terms multiplied by ψ) to the density gradient term. When the wave vector is perpendicular to the magnetic field, $\psi = \nu_e\nu_i/\Omega_e\Omega_i$, and the minimum wavelength for which density gradient effects become important does not change much with altitude.

When L_N is finite, recombination determines the threshold velocity for the excitation of large-scale (tens of meters and larger) gradient drift ($\mathbf{V} = \mathbf{V}_{\perp}$) waves. For $k_{\parallel} = 0$, ψ is small, and $\omega_r = \mathbf{k} \cdot \mathbf{V}_d$, this threshold drift velocity for gradient drift waves, obtained from (11), is

$$V_d = 2\alpha N_0 L_{\text{eff}} \Omega_i \nu_i [1 + \psi(\Omega_i^2 + \nu_i^2)/\nu_i^2]/(\Omega_i^2 + \nu_i^2)$$

Typical values of the recombination time $(2\alpha N_0)^{-1}$ are 15 and 25 s at about 105 and 122 km, respectively. Recombinational damping is most important for wave vectors very close to perpendicular to **B** and for $\Omega_i \sim \nu_i$; ambipolar diffusion rapidly becomes the dominant damping mechanism for short wavelengths and larger aspect angles. In addition, kinetic effects are also important at short wavelengths.

Figure 6 illustrates the variation with wavelength and gradient length of the normalized threshold drift velocity ($\mathbf{k} \cdot \mathbf{V}/kC_s$) obtained by solving (4) for an altitude of about 122 km with the same parameters used for Figure 5 ($2\alpha N_0 = 0.04\ s^{-1}$). Figure 7 shows the variation of the threshold velocity with and without recombinational damping at 122 km. Without such damping, large-scale gradient drift waves could be generated easily when the gradient has the proper sign. As was mentioned above, for waves with **k** perpendicular to the magnetic field the variation of the normalized threshold drift velocity with wavelength does not change much with altitude.

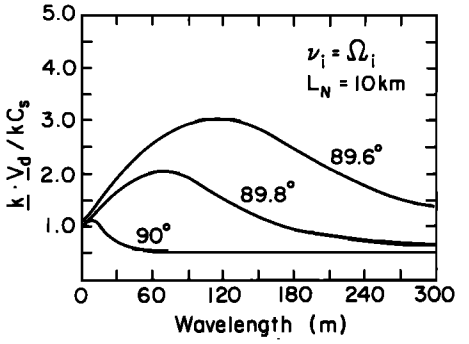

Fig. 8. Variation of the threshold drift velocity with wavelength and aspect angle at 122 km for $2\alpha N_0 = 0.04\ s^{-1}$. These results are not accurate for wavelengths smaller than about 20 m.

The growth rate of the large-scale gradient drift waves is also wavelength independent and maximizes for $k_\parallel = 0$.

Above about 130–140 km the effect of electron-ion collisions cannot be neglected. We can see from (4) that electron collisions affect the dispersion relation only through ψ. When $k_\parallel = 0$, the threshold condition for high-altitude ($\Omega_i \gg \nu_i$) long-wavelength **E** × **B** waves (driven by the ion Pedersen drift) is independent of ψ and is given by $E/BL_{\text{eff}} > 2\alpha N_0$. We neglect nonlocal effects here. At these altitudes, the general dispersion relation with finite density gradient is considerably more complex, particularly for short wavelengths, with $k_\parallel = 0$. However, since the ion Pedersen drift is usually too small to overcome diffusional damping and since kinetic effects are important at short wavelengths, we will not discuss further these high-altitude short-wavelength gradient drift waves. The generation of short-wavelength gradient drift waves in the case of weak electron-neutral collisions was studied by *Gary and Cole* [1983].

The gradient and recombination effects discussed above are valid for $k_\parallel/k < \nu_e/\Omega_e$. This last ratio decreases with increasing altitude and is about 4×10^{-4} where $\Omega_i/\nu_i = 1$. Therefore this limit of $k_\parallel = 0$ may not be of as much practical importance at high altitudes as at low altitudes. For waves with $k_\parallel/k \neq 0$, density gradient and recombination effects are important over a range of aspect angles that decreases with altitude (i.e., decreasing collision frequencies), since ψ is essentially height independent for $k_\parallel/k > \nu_e/\Omega_e$. The variation of the threshold drift velocity with aspect angle with a destabilizing electron density gradient in the upper electrojet region is shown in Figure 8. The shorter wavelengths follow the ion cyclotron threshold, whereas for long wavelengths, density gradient effects decrease the threshold drift.

Ossakow and Chaturvedi [1979] and *Chaturvedi and Ossakow* [1979, 1981] have shown that electron density gradients and field-aligned drifts can excite large-scale (hundreds of meters and larger) current convective waves. The growth rate of these waves can also be obtained from (11), neglecting inertial effects and setting $\mathbf{k} \cdot \mathbf{V}_d = k_\parallel V_\parallel$. The oscillation frequency obtained from (9) is

$$\omega_r = k_\parallel V_\parallel / [1 + \psi(\Omega_i^2 + \nu_i^2)/\nu_i^2]$$

The minimum threshold velocity occurs for

$$k_\parallel^2/k^2 = (\nu_e\nu_i/\Omega_e\Omega_i)[\Omega_i^2/(\Omega_i^2 + \nu_i^2)]$$

For this long-wavelength regime and aspect angle the diffusive damping is very small. Since the recombination coefficient α decreases with increasing altitude, this effect essentially limits the lowest altitude of the unstable layer driven by the current convective instability. For example, at 122 km, using the parameters above with $L_N = 10$ km, the field-aligned threshold velocity is about 28 km s^{-1}. These large-scale current convective waves are driven by field-aligned drifts but have phase velocities determined by the motion of the ambient plasma across the magnetic field lines.

DISCUSSION

Electrojet Waves

These have been discussed in many papers over the last two decades [e.g., *Unwin and Baggaley*, 1972; *Greenwald*, 1974; *Ossakow et al.*, 1975; *Wang and Tsunoda*, 1975; *Moorcroft*, 1979, 1980; *Fejer and Kelley*, 1980; *Schlegel and St.-Maurice*, 1982; *St.-Maurice and Schlegel*, 1983; *Hanuise*, 1983; *Keskinen and Ossakow*, 1983]. We will concentrate here on the effects of electron density gradients and recombination. We have seen that density gradients can decrease or increase considerably the threshold drift velocity for instability when the electric field is parallel or antiparallel to the electron density gradient perpendicular to **B**. Recombinational damping increases the threshold drift velocity for long-wavelength two-stream and gradient drift waves. In the absence of destabilizing density gradients, drift velocities appreciably larger than the ion acoustic speed are needed for the excitation of long-wavelength (tens of meters and larger) waves perpendicular to the magnetic field. Stabilizing gradients have a strong effect even for wavelengths as short as 10 m. These results are in good agreement with recent in situ auroral rocket observations [*Pfaff et al.*, 1984] which indicate a significant decrease of the broadband electron density and electric field fluctuations in a region of stabilizing electron density gradient, even for a drift velocity as large as 1000 m s^{-1}.

Electron density gradients and recombination also play an important role in the generation and characteristics of smaller-scale (wavelengths smaller than about 10 m) secondary irregularities, since these waves are generated by the perturbed velocities and density fluctuations associated with the inferred larger-scale primary waves [e.g., *Sudan et al.*, 1973; *Greenwald*, 1974]. The short-wavelength waves and hence the VHF radar spectra can be affected by density gradients and recombination even when the drift velocity is larger than the ion acoustic speed, since these effects will determine the amplitude of the large-scale waves within which the smaller-scale irregularities exist. This indirect relationship may explain the otherwise puzzling result of *Moorcroft* [1979] that the 398-MHz (corresponding to 38-cm waves) Homer radar did not detect secondary waves whenever the electron density was larger than about 6×10^5 cm^{-3}, in spite of the large electric field (sometimes as much as 50% larger than the normal threshold value) measured simultaneously by the nearby Chatanika radar. For these observations the radar geometry was such that only secondary waves could be observed and the recombination rate $2\alpha N_0$ was about 6 times larger than that used in our calculations for the center of the electrojet (Figure 2). Thus the large-scale waves were heavily damped by recombination.

Waves Above the Electrojet

Rocket observations indicate that the auroral *E* region unstable layer does not extend above about 125–130 km during typical diffuse auroral conditions even for a north-south electric field as large as 54 mV m^{-1}, which corresponds to a drift

velocity of about 1000 m s^{-1} [e.g., *Kelley and Mozer*, 1973; *Pfaff et al.*, 1984]. We have seen that the recombinational damping increases considerably the threshold drift velocity for instability for waves with **k** nearly perpendicular to the magnetic field, particularly in the region where the ion collision frequency and the gyrofrequency are comparable. In addition, for diffuse aurora (electric field nearly parallel to ∇N) the drift velocity of the electrons relative to the ions and the density gradient are nearly antiparallel, so that $L_{\text{eff}} \gg L_N$, which reduces considerably the efficiency of the gradient drift process. Furthermore, as altitude increases, the approximation that $k_\parallel = 0$ is valid only for a very small range of angles, outside of which the effect of density gradients decreases drastically (see Figure 8). A detailed comparison between the results of this theory and data from a number of in situ rocket probes will be presented in a future publication.

We have seen that in the absence of sharp density gradients, large field-aligned electron velocities (tens of kilometers per second) can generate ion cyclotron waves with wavelengths of the order of $2\pi R_i$ (about 20 m for NO^+ and $O_2{}^+$ ions and about 14 m for O^+ ions) only above about 140 km. A threshold drift velocity of 20 km s^{-1} corresponds to field-aligned currents of 32–320 μA m^{-2} if we assume an ambient plasma with a density of 10^4–10^5 cm^{-3} moving with this velocity. Since the electron-ion collision frequency (which decreases the threshold drift velocity) is also proportional to the electron density, very large field-aligned currents and/or additional destabilizing effects which decrease the field-aligned conductivity are needed to excite these waves. In situ satellite and rocket observations have shown the existence of field-aligned drifts large enough to generate these waves in regions where there are large shears in the electric field perpendicular to **B** [*Bering et al.*, 1975; *Burke et al.*, 1983; *Heelis et al.*, 1984]. In addition, there is increasing experimental evidence for ion cyclotron waves measured by in situ rocket probes not only in the *F* region [e.g., *Kelley and Carlson*, 1977] but also in the *E* region [*Ogawa et al.*, 1981; *Yamagishi et al.*, 1981; *Bering*, 1983]. Recently, *Fejer et al.* [1984] presented auroral radar observations which also strongly suggest the occurrence of 3-m ion cyclotron waves above about 140 km. In this case the resonance frequency corresponded to O^+ ion cyclotron waves or to the second harmonic of NO^+ or $O_2{}^+$ waves. As was mentioned previously, the O^+ waves should be easier to excite at shorter wavelengths. The waves observed by in situ probes and radar measurements come from regions where the theory given above and the measured (or inferred) field-aligned currents indicate that they should be generated.

Recent HF radar observations have shown the frequent existence of meter scale waves in the auroral *F* region [*Hanuise et al.*, 1981; *Baker et al.*, 1983]. These small-scale waves are thought to propagate nearly perpendicular to the magnetic field. Although our theory cannot be directly applied to small-scale *F* region waves, it is clear that the large-scale (tens of meters and larger) waves in the upper *E* region do, in fact, have a phase velocity in the rest frame that corresponds to the **E** × **B** drift whether they are driven by cross-field or field-aligned drifts. This suggests that the small-scale waves are generated by or associated with the larger-scale irregularities.

Summarizing, we have developed a generalized theory for auroral *E* region irregularities. The theory is valid for wavelengths much larger than the ion mean free path or ion Larmor radius, whichever is smaller, and provides a framework for comparision with in situ and radar data over a large range of altitudes. In the upper *E* region, waves with $kR_i > 1$ require the use of kinetic theory. Unfortunately, at present, no such theory is available for the region where the ion collision frequency and the gyrofrequency are comparable.

APPENDIX: DERIVATION OF THE LINEAR DISPERSION RELATION

We initially consider linear perturbations of the ion and electron continuity and momentum equations and Poisson's equation. The first-order continuity and momentum equations are given by

$$\frac{Dn}{Dt} + \nabla \cdot (N\mathbf{v}) + n\nabla \cdot \mathbf{V}_0 + 2\alpha Nn = 0 \tag{A1}$$

$$m\frac{D}{Dt}\mathbf{v} - q\mathbf{v} \times \mathbf{B} + m\nu\mathbf{v} = -q\nabla\phi - \frac{n}{N^2}\nabla P_0 - \frac{KT}{N}\nabla n \tag{A2}$$

Here n, $\mathbf{v}$, p, and ϕ are the perturbations. We neglect velocity shear effects, electron inertia, and ion motion along the magnetic field and consider only nearly field-aligned irregularities ($k_\perp \gg k_\parallel$). The reference frame for the ambient electric and magnetic fields and electron density gradient is shown in Figure 1. We now consider the fluctuations proportional to $\exp[i(\mathbf{k}\cdot\mathbf{r} - \omega t)]$ in the reference frame of the ions. Solving for $N\mathbf{v}$ from the momentum equations and then taking the divergence gives

$$\nabla \cdot (N\mathbf{v}_e) = \frac{k_\perp{}^2}{m_i}(-Ne\phi + nKT_e) \cdot \left[\frac{\psi}{\nu_i} - \frac{i}{\Omega_i k_\perp{}^2}\mathbf{k}_\perp \cdot \left(\frac{\nabla N}{N} \times \mathbf{b}\right) - i\frac{\nu_e}{\Omega_e\Omega_i}\frac{\mathbf{k}_\perp \cdot \nabla N}{k_\perp{}^2 N}\right] \tag{A3}$$

$$\begin{aligned}\nabla \cdot (N\mathbf{v}_i) = \frac{k_\perp{}^2}{m_i[\Omega_i{}^2 + (\nu_i - i\omega)^2]}\Bigg\{ & Ne\phi\left[(\nu_i - i\omega) + i\frac{\mathbf{k}_\perp \cdot (\nabla N \times \mathbf{b})\Omega_i}{k_\perp{}^2 N} - \frac{i\mathbf{k}_\perp \cdot \nabla N}{k_\perp{}^2 N}(\nu_i - i\omega)\right] \\ & + nKT_i\left[(\nu_i - i\omega) + i\frac{\mathbf{k}_\perp \cdot (\nabla N \times \mathbf{b})\Omega_i}{k_\perp{}^2 N} + i\frac{\mathbf{k}_\perp \cdot \nabla N}{k_\perp{}^2 N}(\nu_i - i\omega)\right]\Bigg\}\end{aligned} \tag{A4}$$

where

$$\psi = \frac{\nu_e\nu_i}{\Omega_e\Omega_i}\left[1 + \frac{\Omega_e{}^2}{\nu_e{}^2}\frac{k_\parallel{}^2}{k^2}\right]$$

and $\mathbf{b} = \mathbf{B}/B$. Substituting (A3) and (A4) into the electron and ion continuity equations and assuming quasi-neutrality, i.e., $n_e = n_i$, and with $k_\perp{}^2 \gg \mathbf{k}\cdot\nabla N/N$, the dispersion relation can be written as

$$\begin{aligned}(\bar{\omega} - \mathbf{k}\cdot\mathbf{V}_d)\left[\nu_i - i\left(\omega - \frac{\mathbf{k}_\perp \cdot (\nabla N \times \mathbf{b})\Omega_i}{k_\perp{}^2 N}\right)\right] & + \left\{\bar{\omega}[\Omega_i{}^2 + (\nu_i - i\omega)^2] + ik^2 C_s \cdot \left[\nu_i - i\omega + i\frac{\mathbf{k}_\perp \cdot (\nabla N \times \mathbf{b})\Omega_i}{k_\perp{}^2 N}\right]\right\} \\ & \cdot \left(\frac{\psi}{\nu_i} - i\frac{\mathbf{k}_\perp \cdot (\nabla N \times \mathbf{b})}{k_\perp{}^2 N\Omega_i}\right) = 0\end{aligned} \tag{A5}$$

where $\bar{\omega} = \omega + 2i\alpha N$ and the drift velocity $\mathbf{V}_d = \mathbf{V}_e - \mathbf{V}_i$ is

$$\mathbf{V}_d = \left[1 - \frac{\Omega_i^2}{\Omega_i^2 + \nu_i^2}\right]\frac{\mathbf{E}\times\mathbf{B}}{B^2} - \left[\frac{\nu_e}{\Omega_e} + \frac{\nu_i\Omega_i}{\Omega_i^2 + \nu_i^2}\right]\frac{\mathbf{E}}{B} + V_\parallel \mathbf{a}_z \tag{A6}$$

We define $kN/\mathbf{k}\cdot(\nabla N \times \mathbf{b})$ to be L_{eff}, which reduces to $L_N = N \sec\theta(\partial N/\partial h)^{-1}$ when $\mathbf{k}$ is perpendicular to $\mathbf{B}$, giving (4) of the text. The dispersion relation in the rest frame is obtained by substituting $\omega^* - \mathbf{k}\cdot\mathbf{V}_i$ for ω.

Acknowledgments. We thank J.-P. St.-Maurice for helpful discussions and E. Bonelli for help with the computations. This work was supported by the Aeronomy Program of the National Science Foundation through grant ATM-8309662 and by the National Aeronautics and Space Administration under grant NGR-33-010-161.

The Editor thanks J.-P. St.-Maurice and P. K. Chaturvedi for their assistance in evaluating this paper.

REFERENCES

Baker, K. B., R. A. Greenwald, and R. T. Tsunoda, Very high latitude *F* region irregularities observed by HF-radar backscatter, *Geophys. Res. Lett., 10*, 904, 1983.

Bering, E. A., Apparent electrostatic ion cyclotron waves in the diffuse aurora, *Geophys. Res. Lett., 10*, 647, 1983.

Bering, E. A., M. C. Kelley, and F. S. Mozer, Observations of an intense field-aligned thermal flow and associated intense narrow band electric field oscillations, *J. Geophys. Res., 80*, 4612, 1975.

Burke, W. B., M. Silevitch, and H. Hardy, Observations of small-scale auroral vortices by the S3-2 satellite, *J. Geophys. Res., 88*, 3127, 1983.

Chaturvedi, P. K., Collisional ion cyclotron waves in the auroral ionosphere, *J. Geophys. Res., 81*, 6169, 1976.

Chaturvedi, P. K., and P. K. Kaw, Current driven ion cyclotron waves in collisional plasma, *Plasma Phys., 17*, 447, 1975.

Chaturvedi, P. K., and S. L. Ossakow, Nonlinear stabilization of the current convective instability in the diffuse aurora, *Geophys. Res. Lett., 6*, 957, 1979.

Chaturvedi, P. K., and S. L. Ossakow, The current convective instability as applied to the auroral ionosphere, *J. Geophys. Res., 86*, 4811, 1981.

D'Angelo, N., Type III spectra of the radio aurora, *J. Geophys. Res., 78*, 3987, 1973.

Farley, D. T., A plasma instability resulting in field-aligned irregularities in the ionosphere, *J. Geophys. Res., 68*, 6083, 1963.

Farley, D. T., and B. G. Fejer, The effect of the gradient drift term on the type 1 electrojet irregularities, *J. Geophys. Res., 80*, 3087, 1975.

Fejer, B. G., and M. C. Kelley, Ionospheric irregularities, *Rev. Geophys. Space Phys., 18*, 401, 1980.

Fejer, B. G., D. T. Farley, B. B. Balsley, and R. F. Woodman, Vertical structure of the VHF backscattering region in the equatorial electrojet and the gradient drift instability, *J. Geophys. Res., 80*, 1313, 1975.

Fejer, B. G., R. W. Reed, D. T. Farley, W. E. Swartz, and M. C. Kelley, Ion cyclotron waves as a possible source of resonant auroral radar echoes, *J. Geophys. Res., 89*, 187, 1984.

Gary, S. P., and T. E. Cole, Pedersen density drift instabilities, *J. Geophys. Res., 88*, 10,104, 1983.

Greenwald, R. A., Diffuse radar aurora and the gradient drift instability, *J. Geophys. Res., 79*, 4807, 1974.

Hanuise, C., High-latitude ionospheric irregularities: A review of recent radar results, *Radio Sci., 18*, 1093, 1983.

Hanuise, C., J. P. Villain, and M. Crochet, Spectral studies of *F* region irregularities in the auroral zone, *Geophys. Res. Lett., 8*, 1083, 1981.

Heelis, R. A., J. D. Winningham, M. Sugiura, and N. C. Maynard, Particle acceleration parallel and perpendicular to the magnetic field observed by DE 2, *J. Geophys. Res., 89*, 3893, 1984.

Huba, J. D., S. L. Ossakow, P. Satyanarayana, and P. N. Guzdar, Linear theory of the $\mathbf{E}\times\mathbf{B}$ instability with an inhomogeneous electric field, *J. Geophys. Res., 88*, 425, 1983.

Kelley, M. C., and C. W. Carlson, Observations of intense velocity shear and associated electrostatic waves near an auroral arc, *J. Geophys. Res., 82*, 2343, 1977.

Kelley, M. C., and F. S. Mozer, Electric field and plasma density fluctuations due to the high-frequency Hall current two-stream instability in the auroral *E* region, *J. Geophys. Res., 78*, 2214, 1973.

Keskinen, M. J., and S. L. Ossakow, High-latitude ionospheric irregularities: A review, *Radio Sci., 18*, 1077, 1983.

Kudeki, E., D. T. Farley, and B. G. Fejer, Long wavelength irregularities in the equatorial electrojet, *Geophys. Res. Lett., 9*, 684, 1982.

Moorcroft, D. R., Dependence of radio aurora at 398 MHz on electron density and electric field, *Can. J. Phys., 57*, 687, 1979.

Moorcroft, D. R., Comparison of radio-auroral characteristics at 398 MHz with incoherent scatter measurements of electric field, *Can. J. Phys., 58*, 232, 1980.

Ogawa, T., H. Mori, S. Miyazaki, and H. Yamagishi, Electrostatic plasma instabilities in highly active aurora observed by sounding rocket S-310JA-7, *Mem. Natl. Inst. Polar Res. Spec. Issue Jpn., 18*, 321, 1981.

Ossakow, S. L., and P. K. Chaturvedi, Current convective instability in the diffuse aurora, *Geophys. Res. Lett., 6*, 332, 1979.

Ossakow, S. L., K. Papadopoulos, J. Owens, and T. Coffey, Parallel propagation effects on the type I electrojet instability, *J. Geophys. Res., 80*, 141, 1975.

Pfaff, R., M. C. Kelley, B. G. Fejer, E. Kudeki, C. W. Carlson, and A. Pedersen, Electric field and plasma density measurements in the auroral electrojet, *J. Geophys. Res., 89*, 236, 1984.

Schlegel, K., Interpretation of auroral radar experiments using a kinetic theory of the two-stream instability, *Radio Sci., 18*, 108, 1983.

Schlegel, K., and J.-P. St.-Maurice, Note on the parallel propagation effects of unstable Farley-Buneman waves at high latitudes, *Planet. Space Sci., 30*, 315, 1982.

St.-Maurice, J.-P., and K. Schlegel, A theory of coherent radar spectra in the auroral *E* region, *J. Geophys. Res., 88*, 4087, 1983.

Sudan, R. N., Unified theory of the type I and type II irregularities in the equatorial electrojet, *J. Geophys. Res., 88*, 4853, 1983.

Sudan, R. N., J. Akinrimisi, and D. T. Farley, Generation of small-scale irregularities in the equatorial electrojet, *J. Geophys. Res., 78*, 240, 1973.

Unwin, R., and W. J. Baggaley, The radio aurora, *Ann. Geophys., 28*, 111, 1972.

Wang, T. N. C., and R. T. Tsunoda, On a crossed field two-stream plasma instability in the auroral plasma, *J. Geophys. Res., 80*, 2172, 1975.

Watt, T. M., L. L. Newkirk, and E. G. Shelley, Joint radar-satellite determination of the effective recombination coefficient in the auroral *E* region, *J. Geophys. Res., 79*, 4725, 1974.

Yamagishi, H., H. Fukunishi, T. Hirasawa, and T. Ogawa, Measurement of auroral electric fields with an Antartic sounding rocket S-310Ja-7, 2, ac electric field, *Mem. Natl. Inst. Polar Res. Spec. Issue Jpn., 18*, 379, 1981.

D. T. Farley, B. G. Fejer, and J. Providakes, School of Electrical Engineering, Cornell University, Phillips Hall, Ithaca, NY 14853.

(Received February 8, 1984;
revised May 9, 1984;
accepted May 11, 1984.)